IBRO Reports 9 (2020) 14–23

Contents lists available at ScienceDirect

IBRO Reports

journal homepage: www.elsevier.com/locate/ibror

Research Paper

Prenatal exposure to nicotine disrupts synaptic network formation by inhibiting spontaneous correlated wave activity

Yoko Momose-Sato[a,*], Katsushige Sato[b]

[a] Department of Nutrition and Dietetics, College of Nutrition, Kanto Gakuin University, Kanazawa-ku, Yokohama, 236-8501, Japan
[b] Department of Health and Nutrition Sciences, Faculty of Human Health, Komazawa Women's University, Inagi-shi, Tokyo, 206-8511, Japan

ARTICLE INFO

Keywords:
Optical recording
Voltage-sensitive dye
Spontaneous activity
Nicotine
In ovo
Synaptic network formation

ABSTRACT

Correlated spontaneous activity propagating over a wide region of the central nervous system is expressed during a specific period of embryonic development. We previously demonstrated using an optical imaging technique with a voltage-sensitive dye that this wave-like activity, which we referred to as the depolarization wave, is fundamentally involved in the early process of synaptic network formation. We found that the *in ovo* application of bicuculline/strychnine or *d*-tubocurarine, which blocked the neurotransmitters mediating the wave, significantly reduced functional synaptic expression in the brainstem sensory nucleus. This result, particularly for *d*-tubocurarine, an antagonist of nicotinic acetylcholine receptors, suggested that prenatal nicotine exposure associated with maternal smoking affects the development of neural circuit formation by interfering with the correlated wave. In the present study, we tested this hypothesis by examining the effects of nicotine on the correlated activity and assessing the chronic action of nicotine *in ovo* on functional synaptic expression along the vagal sensory pathway. *In ovo* observations of chick embryo behavior and electrical recording using *in vitro* preparations showed that the application of nicotine transiently increased embryonic movements and electrical bursts associated with the wave, but subsequently inhibited these activities, suggesting that the dominant action of the drug was to inhibit the wave. Optical imaging with the voltage-sensitive dye showed that the chronic exposure to nicotine *in ovo* markedly reduced functional synaptic expression in the higher-order sensory nucleus of the vagus nerve, the parabrachial nucleus. The results suggest that prenatal nicotine exposure disrupts the initial formation of the neural circuitry by inhibiting correlated spontaneous wave activity.

1. Introduction

Brain development is strongly affected by environmental factors, particularly during the critical period when brain differentiation and maturation are the most sensitive to perturbation (Thompson et al., 2009; Li et al., 2012; Heindel et al., 2015). Fetal exposure to drugs, alcohol, hormones, and toxicants may alter brain development, thereby increasing the risk of neurological and psychological diseases in postnatal life. Nicotine in cigarettes is a major environmental factor that disrupts normal brain development (Slotkin, 2004; Dwyer et al., 2009). Nicotine exerts its effects by interfering with nicotinic acetylcholine receptors (nAChRs), which regulate numerous processes of neural development, including gene expression, cell death, synaptogenesis, the regulation of neurotransmitter release, and plasticity events (Nguyen et al., 2001; Dajas-Bailador and Wonnacott, 2004).

In the developing nervous system, nAChRs mediate correlated spontaneous activity in the developing brain-spinal cord. This activity has been referred to as network-driven activity (O'Donovan, 1999), spontaneous network activity (Gonzalez-Islas and Wenner, 2006), and rhythmic spontaneous neural activity (Vincen-Brown et al., 2016). In our optical imaging study with voltage-sensitive dyes, this activity exhibited unique wave-like propagation over a wide region of the central nervous system, maximally extending to the lumbosacral cord and forebrain (Momose-Sato et al., 2007; Momose-Sato et al., 2009; Momose-Sato et al., 2012a). Based on this profile, we referred to this activity as the depolarization wave (for reviews, Momose-Sato and Sato, 2013; Momose-Sato and Sato, 2016a). Pharmacological studies revealed that the generation and propagation of this activity were

Abbreviations: APV, $_{DL}$-2-amino-5-phosphonovaleric acid; CNQX, 6-cyano-7-nitroquinoxaline-2,3-dione; E, embryonic day (days of incubation in avians and days of pregnancy in mammals); EPSP, excitatory postsynaptic potential; GABA, γ-aminobutyric acid; nAChR, nicotinic acetylcholine receptor; NMDA, *N*-methyl-$_{D}$-aspartate; NTS, nucleus of the tractus solitarius; PBN, parabrachial nucleus

* Corresponding author at: Department of Nutrition and Dietetics, College of Nutrition, Kanto Gakuin University, 1-50-1 Mutsuura-Higashi, Kanazawa-ku, Yokohama, 236-8503, Japan.
E-mail address: yms@kanto-gakuin.ac.jp (Y. Momose-Sato).

https://doi.org/10.1016/j.ibror.2020.06.003
Received 23 April 2020; Accepted 20 June 2020

dominantly mediated by acetylcholine at early stages, which was later replaced by glutamatergic networks (Nakayama et al., 1999; Ren and Greer, 2003; Ladle et al., 2007; Mochida et al., 2009; Momose-Sato et al., 2012b).

Correlated activity, termed the depolarization wave, has been observed in many species, including birds and rodents (Momose-Sato and Sato, 2013; Momose-Sato and Sato, 2016a). Although there is considerable consensus on the global features of wave activity, its physiological significance remains unclear. Previous studies that focused on the spinal cord reported that correlated spontaneous activity may be fundamentally involved in the formation of spinal motor circuits (Hanson and Landmesser, 2004; Kastanenka and Landmesser, 2010; Gonzalez-Islas and Wenner, 2006; Wilhelm et al., 2009) and the development of locomotor functions (Myers et al., 2005). However, the role of this activity in the brain and the significance of large-scale propagation have not yet been elucidated.

The wide propagation of the correlated wave over the brain and spinal cord is observed during a specific period of embryogenesis (Momose-Sato et al., 2009; Momose-Sato et al., 2012a; Momose-Sato and Sato, 2014), at which functional synaptic contacts are initially expressed in the brainstem and spinal cord (Lee et al., 1988; Mochida et al., 2001; Momose-Sato et al., 2001, 2015; Glover et al., 2008). This finding suggests that the wave regulates the initial process of synaptic network organization. In our previous study, we tested this hypothesis by chronically inhibiting the wave and examining its effects on functional synaptic expression in the brainstem sensory nucleus (Momose-Sato and Sato, 2017). The *in ovo* application of bicuculline/strychnine or *d*-tubocurarine, which inhibited the wave, markedly reduced synaptic responses in the second-order nucleus of the vagal sensory pathway, the parabrachial nucleus, demonstrating that the wave plays a fundamental role in synaptic network formation (Momose-Sato and Sato, 2017).

This finding, particularly for *d*-tubocurarine, an antagonist of nAChRs, led to a new hypothesis that prenatal exposure to nicotine associated with maternal smoking affects the development of neural circuit formation by interfering with correlated wave activity. A more detailed understanding of the mechanisms underlying the toxic effects of nicotine on neural development will contribute to the prevention of fetal disorders caused by maternal smoking during pregnancy. In the present study, we tested this new hypothesis by examining the effects of nicotine on correlated wave activity and assessing the chronic effects of nicotine on functional synaptic expression.

The preliminary results obtained were previously reported in abstract form (Momose-Sato and Sato, 2019).

2. Materials and methods

2.1. Ethics

Experiments were approved by the Ethics Committees of Kanto Gakuin University and Komazawa Women's University, and were performed in accordance with the Japan Society for the Promotion of Science guidelines and the National Institute of Health Guide for the Care and Use of Laboratory Animals. All efforts were made to minimize the number of animals used and their suffering.

2.2. In ovo application of drugs

Procedures for the *in ovo* application of drugs were similar to those described previously (Momose-Sato and Sato, 2017). Fertilized eggs of White Leghorn chickens were obtained from Shiraishi Laboratory Animals, Saitama, Japan, and were incubated at 38 °C and 60 % humidity. Correlated wave activity in the chick embryo appears from E (embryonic day: days of incubation) 3.5–4 (Hamburger and Balaban, 1963; Milner and Landmesser, 1999; Hanson and Landmesser, 2004; Momose-Sato et al., 2009), and is mediated by nAChRs at early stages (~E6) and glutamate receptors at later stages (E6~), while it also depends on the excitatory effects of GABA (γ-aminobutyric acid) and glycine at all stages (Milner and Landmesser, 1999; Hanson and Landmesser, 2004; Mochida et al., 2009). To examine the acute effects of *d*-tubocurarine or nicotine *in ovo*, a window in the shell was opened at E5-E7, and *d*-tubocurarine or nicotine [1 − 5 mM (mostly 5 mM) in 100 μL of Ringer's solution (see the Section 2.3) containing penicillin (100 unit/mL)/streptomycin (0.1 mg/mL)] was added to the embryo (n = 20 at E5, n = 12 at E6, n = 14 at E7). The concentration of the drug *in ovo* was estimated to be 2–10 μM, assuming that the egg volume was 50 mL and the drug (1 − 5 mM, 100 μL) diffused uniformly within the egg. The concentration around the embryo appeared to be marked higher just after the administration of the drug. The tissue over the fourth ventricle is thin in the early stages, and, thus, it is reasonable to assume that the drug diffused well into the brainstem; however, the exact concentration of the drug within the brain remains unknown. Embryonic movements before and after drug application were monitored with the naked eye and a video camera set on a dissecting microscope.

To examine the chronic effects of nicotine on functional synaptic expression, a window in the shell was opened at E4 and nicotine was applied once a day from E4 to E7. After the daily application of nicotine, the shell window was sealed with paraffin film, and the incubation was continued. The procedures used for the *in ovo* application of drugs, including removal of the shell membrane, often damaged fine vessels, which resulted in a high incidence of embryo death. The survival rate of embryos with the chronic application of nicotine was 62.4 % (n = 93) at E8, whereas that with the application of Ringer's solution without the drug (100 μL/day) was 42.0 % (n = 69) at E8. The survival rate of embryos was significantly higher with the application of nicotine than with Ringer's solution ($\chi^2(1) = 6.59$, $P = 0.01$). The reason for this difference remains unknown; however, this result suggests that the toxic effects of nicotine were negligible in relation to the survival rate of embryos. Since nicotine experiments were performed after those with Ringer's solution, improvements in the surgical techniques performed may underlie the observed result.

2.3. Preparation for electrical recording

Fertilized eggs were incubated for 5–6 days (E5-E6). ICR mice and Wistar rats were obtained from Nippon Bio-Supply Center, Tokyo, Japan. Females were caged with males in the evening and checked for sperm the next morning: this day was termed E0. Pregnant mice or rats at E12-E13 gestation were anesthetized with ether or isoflurane, and the spinal cord was dislocated at the cervical level. Their fetuses were then surgically removed. The brainstem-spinal cord preparation was dissected from E5-E6 chicks (n = 13), E12-E13 mice (n = 25), and E13 rats (n = 6) in ice-cold solution. Chick preparations were kept in Ringer's solution that contained the following (in mM): NaCl, 138; KCl, 5.4; $CaCl_2$, 1.8; $MgCl_2$, 0.5; Tris-HCl buffer (pH 7.3), 10; and glucose, 10, equilibrated with oxygen, and those of mice and rats were kept in artificial cerebrospinal fluid (ACSF) that contained the following (in mM): NaCl, 124; KCl, 5; $CaCl_2$, 2.5; $MgSO_4$, 1; NaH_2PO_4, 1.25; $NaHCO_3$, 22; and glucose, 10, equilibrated with a mixture of 95 % O_2 and 5% CO_2 (pH 7.4). These preparations were placed in a recording chamber and superfused with the bathing solution at 1 − 2 ml/min at 28 ± 1 °C until spontaneous activity was stably recorded by electrophysiological means (see the Section 2.4).

2.4. Electrical recording of spontaneous cranial and spinal nerve discharges

Spontaneous correlated activity was monitored as the electrical discharges of recruited vagal and/or spinal motoneurons. Glass microsuction electrodes were applied to the cut end of the vagus and/or lumbar spinal nerve roots. Electrical signals were amplified with filters set at 0.08 Hz and 1 kHz, and then digitally recorded at 4 kHz using an analog-to-digital converter (MacLab/8S, ADInstruments, Castle Hill,

Australia).

2.5. Preparation for optical recording

Fertilized eggs were incubated for 8 days (E8) with or without the nicotine treatment *in ovo*. To assess the chronic effects of nicotine, we examined the development of vagal sensory nuclei using a previously described method (Momose-Sato and Sato, 2017). At E8, chick embryos were isolated and decapitated, and *en bloc* brainstem preparations with the vagus nerve attached were dissected in ice-cold Ringer's solution. The dorsal midline of the cerebellum and midbrain was cut, and the preparation was flattened bilaterally reflecting the cerebellum and midbrain. Slice preparations (thickness of approximately 1,500 μm) were made by transecting isolated brainstems at the level of the vagus nerve root. The chronic application of the drug *in ovo* sometimes inhibited embryonic growth, and this appeared to be because the loss of motor outputs associated with correlated activity caused muscle paralysis and a deficit in muscle and bone development (Roufa and Martonosi, 1981; Persson, 1983; Hall and Herring, 1990). To exclude the effects of growth retardation, the results obtained with nicotine were compared with those from control embryos at the same stage, and underdeveloped or malformed embryos were discarded. We performed optical analyses using embryos at stages 33–34 in *en bloc* preparations and stage 33 in slice preparations. The meningeal tissue of the brainstem preparation was removed, and the preparation was stained with the voltage-sensitive merocyanine-rhodanine dye, NK2761 (0.2 mg/mL, 10−15 min staining) (Hayashibara Biochemical Laboratories Inc./Kankoh-Shikiso Kenkyusho, Okayama, Japan: Salzberg et al., 1983; Kamino et al., 1981; Momose-Sato et al., 1995). The usefulness of this dye for staining embryonic nervous and cardiac tissues was previously demonstrated (Kamino, 1991; Momose-Sato et al., 1995, 2015). After staining, the preparation was placed in a recording chamber with the ventral side up for *en bloc* preparations or spinal cord side up for slice preparations. The vagus nerve was stimulated with a glass microsuction electrode (8 μA/5 msec, single shot) to evoke excitatory postsynaptic potentials (EPSPs) in vagal sensory nuclei. The preparation was superfused with Ringer's solution at 1−2 ml/min at room temperature (24−28 °C), except for at the time of data acquisition.

2.6. Optical recording of vagal postsynaptic responses

The optical recording method used in the present study was similar to that reported previously (Momose-Sato and Sato, 2016b, 2017). In brief, incident light provided by a 300-W tungsten-halogen lamp powered by a stable dc-power supply was collimated and rendered quasi-monochromatic using an interference filter with a transmission maximum of 699 ± 13 nm (half-width) (Asahi Spectra Co., Tokyo, Japan). The objective (×10, 0.4 NA) and photographic eyepiece (×2.5) lenses projected an image of the preparation onto a silicon photodiode array mounted on a microscope. The focus was set to the preparation surface; however, the optical signals included responses from every depth because the loose structure of the embryonic tissue allowed the dye to diffuse readily into the deeper regions and consequently stain neurons relatively well (Sato et al., 1995), and activity in the dorsal brainstem nucleus was detected from the ventral side (Momose-Sato et al., 1991). In absorption measurements, Z-axis resolution was not sufficient to discriminate neuronal responses in the focal plane from those out of focus, as reported in the barnacle ganglion with changes in the focal plane (Salzberg et al., 1977). Changes in the transmitted light intensity through the preparation were detected with the photodiode array (34 × 34 elements) and were recorded using a 1,020-site optical recording system constructed in our laboratory (Hirota et al., 1995; Momose-Sato et al., 2015). All recordings were made in single sweeps without averaging.

2.7. Blockers

In pharmacological experiments, *d*-tubocurarine was acquired from Wako Pure Chemical Industries Ltd. (Osaka, Japan), nicotine and $_{DL}$-2-amino-5-phosphonovaleric acid (APV) from Sigma Chemical Co. (St. Louis, MO, USA), and 6-cyano-7-nitroquinoxaline-2,3-dione (CNQX) from Research Biochemicals International (Natic, MA, USA).

2.8. Data analysis

In optical recordings, the fractional change in dye absorption, ΔA/A, is proportional to the change in membrane potentials. ΔA/A is equal to $-\Delta I/(I_{\text{before staining}}-I_{\text{after staining}})$, where I is the light intensity transmitted through the preparation (Ross et al., 1977). In the embryonic brainstem preparation, regional variations in $I_{\text{after staining}}/I_{\text{before staining}}$ were small (Momose-Sato and Sato, 2006). Thus, we measured $I_{\text{after staining}}$ and ΔI, and expressed the optical signal as $-\Delta I/I_{\text{after staining}}$, which was assumed to be proportional to ΔA/A. Color-coded images of the optical signals were constructed using the "NeuroPlex" program (RedShirtImaging LLC, Fairfield, CT, USA). In quantitative analyses, results were expressed as the mean ± standard error of the mean (SEM). When maximum -ΔI/I was less than 1.0×10^{-4}, optical responses were not significant, and the signal size was evaluated as 0. In statistical analyses of signal amplitude, any differences were tested using the unpaired *t*-test (two-tailed) in Excel (ver. 14.7.1, Microsoft, Tokyo, Japan). We tested for and found normal distributions and equal variances in sampled data. "t" shows the statistic's value (t ratio) together with the degree of freedom. "*d*" indicates Cohen's *d* value (effect size). The survival rates of embryos with the chronic application of nicotine and Ringer's solution were compared using the chi-squared test (StatPlus:mac Pro, ver. 7.1.30, AnalystSoft Inc., CA, USA). "χ^2" shows the statistic's value together with the degree of freedom. "n" indicates the number of data points. "*P*" means the *P*-value. Significance in statistical analyses was accepted at P values < 0.05.

3. Results

3.1. Evaluation of acute effects of nicotine

To examine whether nicotine applied *in ovo* affected spontaneous correlated wave activity, we monitored embryonic motility, which is generated by coordinated cranial and spinal motoneuronal discharges associated with correlated wave activity (Momose-Sato and Sato, 2013; Momose-Sato and Sato, 2016a). Embryonic motility initially appears at E3.5-E4 as slight flexion of the neck to the left and right, and later exhibits S-waves extending from the head to the level of the tail (Hamburger and Balaban, 1963; Provine, 1973; Bekoff et al., 1975). The pattern of embryonic motility does not markedly change during E4-E7, except for the number of successions, initiation sites, and contribution of the wings and legs (Hamburger and Balaban, 1963). Although embryonic movements are observed beyond the stage at which the large-scale correlated wave is detected (E4-E8) (Momose-Sato and Sato, 2016a), they are associated with reflexogenic activity that appears from E7-E7.5 (Hamburger and Balaban, 1963), respiratory and locomotor functions that differentiate later than correlated wave activity (Branchereau et al., 2000; Thoby-Brisson et al., 2005, 2009; Momose-Sato et al., 2012a), and sleeping behavior (Corner, 1977). Since the purpose of the *in ovo* application of nicotine was to affect the wave during E4-E7, we targeted wave-related body movement observed in earlier stages and did not perform detailed analyses on embryonic motility in later stages.

Fig. 1A shows raster diagrams of embryonic movements (vertical lines) observed *in ovo* at E5 and E6. Embryonic motility consisting of single or multiple bursts appeared spontaneously and periodically (also see Video 1). When *d*-tubocurarine (5 mM, 100 μL) was applied, motility was eliminated with no change in the heart rate (Fig. 1B). Similar

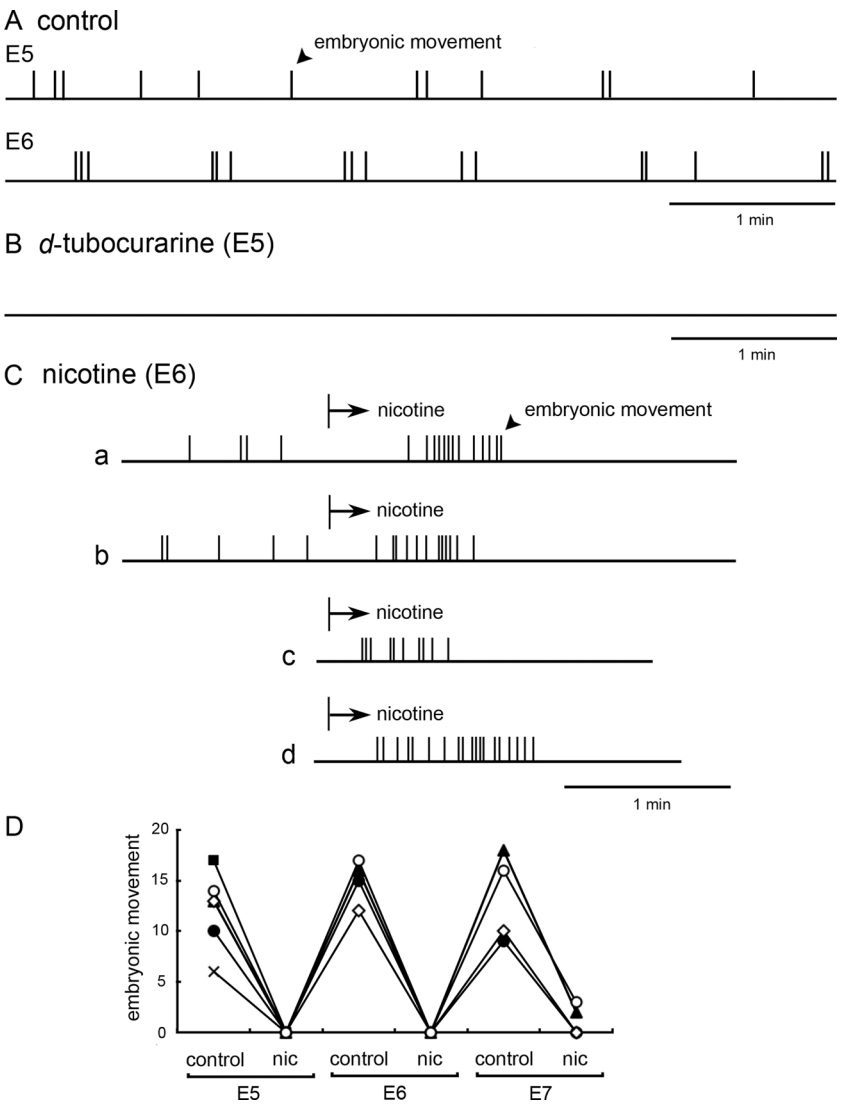

Fig. 1. Effects of nicotine on embryonic movements *in ovo*. **A,** Raster diagrams of the spontaneous movements of chick embryos observed at E5 and E6 *in ovo*. A window in the shell was opened each day, and body flexions of the embryo (vertical lines) were monitored with the naked eye and a video camera set on a dissecting microscope. **B,** Embryonic motility was eliminated by the *in ovo* application of *d*-tubocurarine (5 mM, 100 μL). The recording was made at E5. **C,** Raster diagrams of spontaneous embryonic movements in response to the *in ovo* application of nicotine (5 mM, 100 μL). Four examples of E6 embryos are shown. Embryonic movements transiently increased just after the application of nicotine, but were subsequently inhibited. **D,** Monitoring of embryonic movements through E5 to E7. Nicotine (5 mM, 100 μL) was applied *in ovo* once a day, and the number of embryonic movements was counted for 5 min before (control) and after (nic) the application of nicotine. Each symbol corresponds to one embryo.

results for *d*-tubocurarine were obtained in 4/4 embryos at E5, 2/3 embryos at E6, and 7/7 embryos at E7 at a concentration of 5 mM, and 5/5 embryos at E5, 1/3 embryos at E6, and 4/4 embryos at E7 at a concentration of 1 mM, while motility in other embryos was slowed, but not completely blocked.

Fig. 1C shows four examples of raster diagrams obtained in response to nicotine. When nicotine (5 mM, 100 μL) was applied *in ovo*, embryonic movements transiently increased, but were followed by the elimination of motility (Fig. 1C, Video 2). Motility did not recover during the period of monitoring (5−30 min). Similar results for nicotine were obtained in 6/6 embryos at E5 and 2/3 embryos at E6 at a concentration of 5 mM, and 4/5 embryos at E5, 2/3 embryos at E6, and 2/3 embryos at E7 at a concentration of 1 mM, while motility in other cases was reduced, but not completely eliminated.

The effects of nicotine applied *in ovo* were not permanent, and motility recovered when embryonic movement was monitored one day after the administration of the drug (Fig. 1D). Vincen-Brown et al. (2016) previously reported that prolonged exposure to nicotine *in vitro* (6 h <) caused the reappearance of spontaneous activity through the activation of GABA/glycinergic excitatory networks. In the present study, recovered embryonic motility was again blocked by the same dose of nicotine (Fig. 1D, nic). Thus, the reappearance of motility was not due to compensation of the network generating the activity by other transmitter systems, but to a decrease in the efficiency of nicotine, possibly due to diffusion.

To confirm that nicotine applied *in ovo* affected correlated wave activity generated in the brain, we examined the effects of nicotine in *in vitro* preparations and compared the results obtained with those for embryonic motility. Fig. 2A and B show examples of electrical recordings obtained from isolated chick brainstem-spinal cord preparations. These recordings were made from the vagus nerve (N.X) in the control (Fig. 2A) and in response to nicotine (Fig. 2B). In the control (Fig. 2A), spontaneous activity appeared periodically with episodic discharges containing several bursts (Fig. 2A, arrowheads). This activity was blocked (n = 5) or slowed (n = 2) when *d*-tubocurarine (10 μM) was applied to E5-E6 preparations (data not shown). When nicotine (10 μM) was applied (Fig. 2B, indicated by an arrowhead), bursting activity transiently increased (Fig. 2B, an asterisk), and this was followed by an inhibition of the burst and increase in tonic non-episodic activity. Similar results were obtained from five other preparations dissected from E5-E6 embryos.

In the following sections of the present study, the target of chronic experiments was the chick embryo *in ovo*. Nevertheless, it is of clinical importance to obtain information on the effects of nicotine in mammalian embryos and assess whether these results are homologous among species because this information will be beneficial for discussing social issues caused by maternal smoking and facilitating future research focusing on *in situ* preparations (also see Discussion). Fig. 2C–E show examples of electrical recordings obtained from mouse (Fig. 2C and D) and rat (Fig. 2E) brainstem-spinal cord preparations. In control

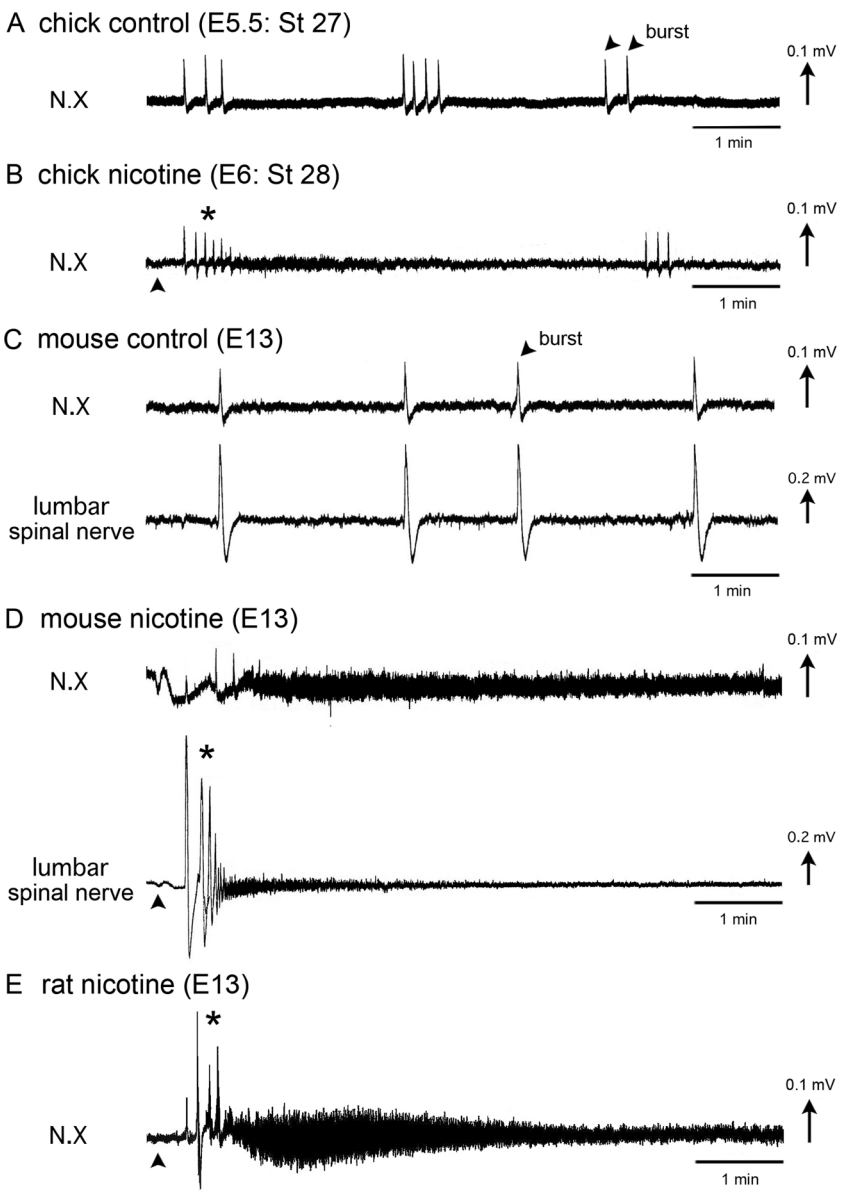

Fig. 2. Effects of nicotine on spontaneous correlated activity *in vitro*.
A, Spontaneous electrical discharges detected from the vagus nerve (N.X) in an E5.5 (stage 27) chick brainstem-spinal cord preparation. Activity exhibited periodic episodes containing several bursts (arrowheads). **B,** Effects of nicotine (10 μM) on spontaneous activity in an E6 (stage 28) chick brainstem-spinal cord preparation. **C,** Spontaneous electrical discharges detected from the vagus nerve (N.X) and lumbar spinal nerve in an E13 mouse brainstem-spinal cord preparation. **D–E,** Effects of nicotine (10 μM) on spontaneous activity in E13 mouse (**D**) and E13 rat (**E**) brainstem-spinal cord preparations. In **B**, **D**, and **E**, nicotine was applied to the bathing solution at the timing indicated with arrowheads. Bursting activity associated with the correlated wave transiently increased just after the application of nicotine (asterisks), but was subsequently inhibited.

recordings obtained from the mouse (Fig. 2C), spontaneous activity appeared with a correlation between the vagus nerve (N.X) and lumbar spinal nerve, demonstrating that this activity widely correlated within the brain and spinal cord. When *d*-tubocurarine (10 μM) was applied, activity was blocked (n = 4) or slowed (n = 1) in E12-E13 preparations (data not shown). The application of nicotine (10 μM) induced a series of bursts, followed by the inhibition of bursts and increase in non-episodic activity in both mouse (Fig. 2D) (n = 4 at E12-E13) and rat (Fig. 2E) (n = 1 at E13) preparations. Similarity, the results obtained from chick, mouse, and rat embryos suggested that the effects of nicotine are homologous among species.

The results shown in Fig. 2 are consistent with previous observations reported in the chick brainstem and spinal cord *in vitro*. Vincen-Brown et al. (2016) reported that nicotine (0.5 μM) applied to isolated chick brainstems at E5 induced a series of electrical bursts of glossopharyngeal nerve (N.IX), followed by the elimination of bursting episodes and an increase in spontaneous unit activity. Milner and Landmesser (1999) also reported that nicotine (10 μM) induced similar changes in spontaneous spinal nerve activity in E6 chick embryos, while nicotine at a lower concentration (0.1 μM) blocked spontaneous bursting without inducing a series of burst. Since correlated wave activity is associated with bursting activity detected electrophysiologically (Milner and Landmesser, 1999; Momose-Sato et al., 2007, 2009, Momose-Sato et al., 2012a; Vincen-Brown et al., 2016), the effects of nicotine *in ovo* paralleled those observed *in vitro*. The results suggest that nicotine applied *in ovo* affected correlated wave activity generated in the brain, although the contribution of nAChRs located outside the brain cannot be excluded.

Nicotine, a ligand of nAChRs, activates and desensitizes nAChRs (Dani and Bertrand, 2007). Thus, it may positively or negatively regulate spontaneous correlated activity. The results shown in Figs. 1 and 2 demonstrated that correlated wave activity was transiently potentiated, but subsequently inhibited by nicotine, the latter of which may have been due to the desensitization of nAChRs and/or desynchronization of neurons recruited into the wave. These results suggest that the positive effects of nicotine on the correlated wave were transient, while the dominant action was to inhibit the wave.

3.2. Evaluation of chronic effects of nicotine on monosynaptic EPSPs

Based on the results obtained with the acute application of nicotine, we examined the effects of the chronic application of nicotine on

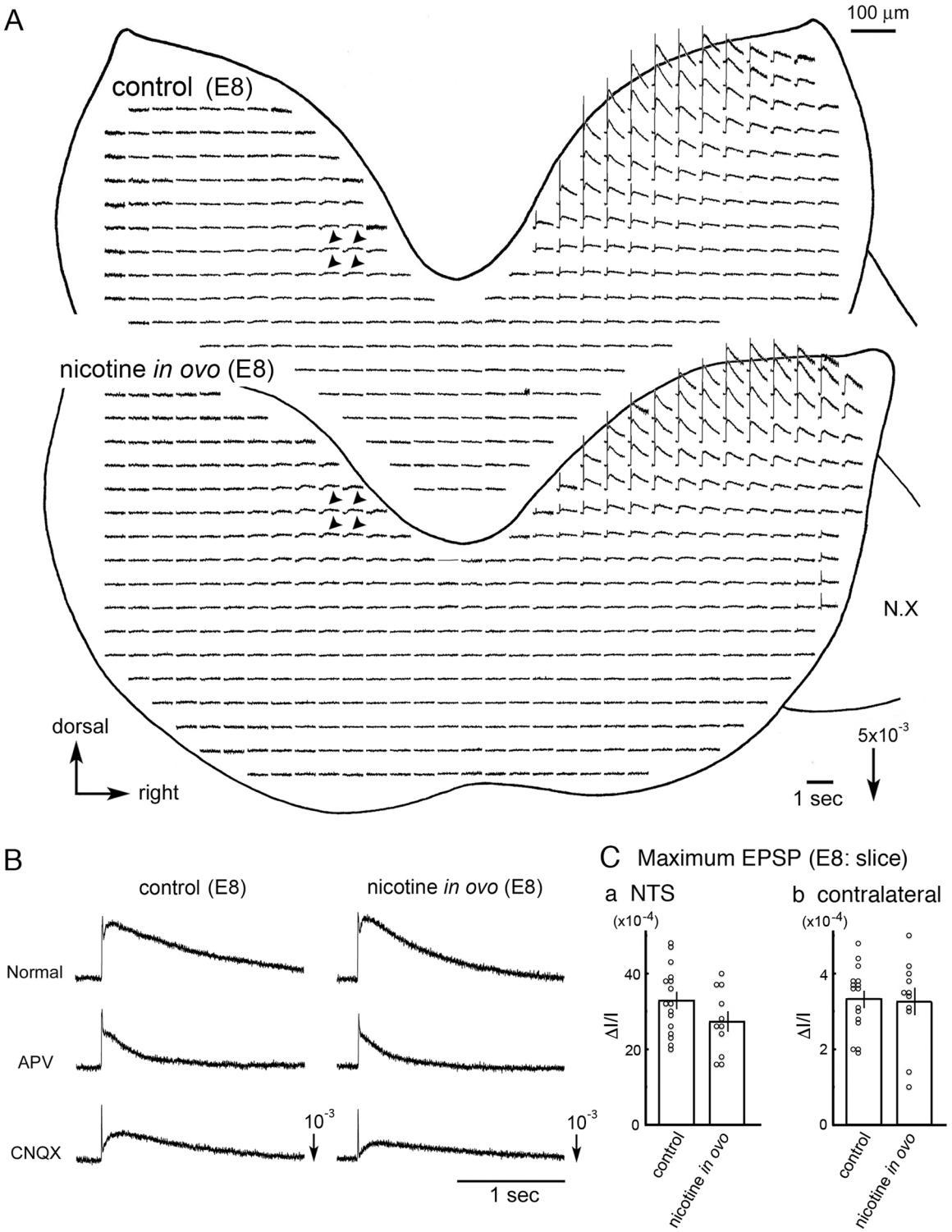

Fig. 3. Evaluation of chronic exposure to nicotine on vagal monosynaptic responses.
A, Multiple-site optical recordings of vagal responses in E8 brainstem slices dissected from embryos with (lower) or without (upper) chronic exposure to nicotine *in ovo* (5 mM, 100 μL/day). Optical signals are arranged according to the positions of the photodiode array elements, and signals from outside the preparation were omitted for clarity. Stimulation was applied to the right vagus nerve (N.X), and monosynaptic EPSPs were detected from the ipsilateral NTS and contralateral non-NTS region (arrowheads). The arrow pointing to the lower right of the recording indicates an increase in the transmitted light intensity (decrease in absorption), and the length of the arrow represents the stated value of the fractional change ΔI/I, the change in light intensity divided by the DC background intensity. The upward direction of the signal corresponds to membrane depolarization. Recordings were obtained in single sweeps. **B,** Enlarged traces of the optical signal recorded in normal (top), APV (200 μM)-containing (middle), and CNQX (5 μM)-containing (bottom) solutions in E8 brainstem slices treated with (right) or without (left) chronic exposure to nicotine *in ovo* (5 mM, 100 μL/day). CNQX was applied to the solution 10 min after the washout of APV. Optical signals were detected in the region corresponding to the NTS. **C,** Histograms showing the maximum amplitude of the EPSP-related slow signal (mean ± SEM) together with each data point (circles) in the NTS (**a**) and contralateral non-NTS region (**b**) of E8 brainstem slices.

synaptic network formation along the vagal sensory pathway. Since the effects of nicotine applied at E4 were not permanent (Fig. 1D), we applied nicotine daily until E7 (5 mM, 100 μL/day), the day before optical recordings.

Optical recordings of vagal responses in E8 brainstem slices with and without the application of nicotine *in ovo* are shown in Fig. 3A. In control preparations (Fig. 3A, upper), the vagal stimulation evoked large optical signals on the ipsilateral side (right side of Fig. 3A), and small signals on the contralateral side (indicated with arrowheads on the left side of Fig. 3A). An enlargement of the optical signal detected from the ipsilateral side is shown in Fig. 3B (top, left trace). The signal consisted of a fast spike-like signal and slow long-lasting signal, which corresponded to the sodium-dependent action potential and glutamatergic EPSP, respectively (Komuro et al., 1991; Momose-Sato et al., 1994). Previous studies reported that the vagal stimulation of the E8 chick embryo induced monosynaptic EPSPs in the ipsilateral nucleus of the tractus solitarius (NTS) and the contralateral non-NTS region (Momose-Sato et al., 1991, 1994; Momose-Sato and Sato, 2005, 2011). The areas in which the slow optical signals were detected in Fig. 3A represent these vagal sensory nuclei.

When similar optical recordings were conducted in an E8 preparation exposed to nicotine *in ovo* (Fig. 3A, lower), the vagal stimulation elicited similar optical responses to those of the control. Enlargements of the optical signal (Fig. 3B, top traces) together with those in the presence of APV (an *N*-methyl-$_D$-aspartate (NMDA) receptor antagonist) and CNQX (a non-NMDA receptor antagonist) (Fig. 3B, second and bottom traces) indicated that components of the optical signal and the pharmacological nature of the EPSP were not qualitatively different from those in the control preparation.

The fractional change in optical signals was proportional to membrane potential changes and the active membrane area detected by one photodiode (Obaid et al., 1985; Orbach et al., 1985; Kamino et al., 1989). Therefore, the amplitude of the slow signal was proportional to the size of EPSPs and number of postsynaptic neurons in the sensory nucleus. To quantitatively examine the effects of nicotine, we evaluated the amplitude of the largest slow signal in each nucleus. Fig. 3C shows the results obtained for the NTS (Fig. 3C-a) and contralateral non-NTS region (Fig. 3C-b). In the NTS (Fig. 3C-a), the mean ± SEM of the maximum EPSP (ΔI/I) was 32.9 ± 2.2 (n = 16) in the control and 27.3 ± 2.6 (n = 11) in preparations treated with nicotine *in ovo*. No significant difference was observed between these groups (t_{25} = 1.65, P = 0.11) (also see the result of *en bloc* preparations shown in Fig. 4C-a). In the contralateral non-NTS region (Fig. 3C-b), the maximum EPSP (ΔI/I) was 3.3 ± 0.2 (n = 16) in the control and 3.3 ± 0.4 (n = 11) in nicotine-treated preparations, and there was no significant difference (t_{25} = 0.13, P = 0.89).

Collectively, these results suggest that the development of functional synapses in the first-order sensory nuclei of the vagus nerve, *i.e.* the NTS and contralateral non-NTS region, was not significantly affected by the chronic application of nicotine *in ovo*, at least until E8.

3.3. Evaluation of chronic effects of nicotine on polysynaptic EPSPs

A major target for ascending projections from the NTS is the parabrachial nucleus (PBN) (Norgren, 1978; Herbert et al., 1990). Polysynaptic responses in the PBN have been identified in the contralateral pons/medulla region in the E8 chick brainstem (Sato et al., 2004). Optical responses in the PBN and NTS in an E8 *en bloc* brainstem preparation are shown in Fig. 4A-a. Vagal responses were detected from two regions corresponding to the level of the NTS (Fig. 4A-a, upper images) and PBN (Fig. 4A-a, lower images), as indicated by squares in the right inset. Enlargements of the optical signals detected from these regions are shown in Fig. 4B-a. Comparisons of signal onsets revealed a marked delay between the signals in the two regions, suggesting that the signal detected from the PBN corresponded to the polysynaptic response *via* the NTS.

When we examined vagal responses in *en bloc* preparations treated with nicotine *in ovo,* optical responses in the NTS were similar to those in the control (Fig. 4A-b, upper images and Fig. 4B-b, upper trace), whereas the signals in the PBN were often small and not significant ($\Delta I/I < 1.0 \times 10^{-4}$) (Fig. 4A-b, lower images and Fig. 4B-b, lower trace). Since recordings were initially made in the PBN followed by the NTS, these results were not due to the time-dependent deterioration of the preparation. In quantitative analyses, the maximum EPSP (ΔI/I) in the NTS of *en bloc* preparations was 13.1 ± 0.9 (n = 19) in the control and 12.8 ± 1.0 (n = 19) in nicotine-treated embryos (Fig. 4C-a). No significant difference was observed between these groups (t_{36} = 0.21, P = 0.83). Whereas, the maximum EPSP (ΔI/I) in the PBN was 2.9 ± 0.3 (n = 21) in the control and 2.1 ± 0.2 (n = 19) in nicotine-treated preparations (Fig. 4C-b), showing that the EPSP in the PBN was significantly reduced by nicotine (t_{38} = 2.40, P = 0.02, d = 0.76).

These results suggest that exposure to nicotine *in ovo* inhibited functional synaptic expression in the higher-order sensory nucleus, resulting in the disruption of synaptic network formation along the sensory pathway.

4. Discussion

4.1. Nicotine inhibited correlated wave activity

The generation of spontaneous activity is one of the important roles of acetylcholine during the early phase of neural development. Propagating wave-like activity in the brain-spinal cord (the activity studied in the present experiment) and that in the retina (termed the retinal wave) (Wong, 1999) is mediated by nAChRs during a specific period of development, which is later replaced by glutamatergic regulation (Nakayama et al., 1999; Ren and Greer, 2003; Ladle et al., 2007; Mochida et al., 2009; Momose-Sato et al., 2012b; Wong, 1999). Regarding nAChR subtypes, previous studies reported that correlated wave activity in the brain-spinal cord was more dominantly dependent on nAChRs containing non-α7 subunits than the α7 subtype (Milner and Landmesser, 1999; Momose-Sato et al., 2012b). Furthermore, Milner and Landmesser (1999) demonstrated that the inhibition of correlated activity by nicotine was prevented by a previous incubation with non-α7 subtype blockers, suggesting that the effects of nicotine were mediated by non-α7 receptors.

Nicotine, a ligand of nAChRs, activates and desensitizes nAChRs (Dani and Bertrand, 2007). Therefore, it may positively or negatively regulate spontaneous correlated wave activity. In the present study, embryonic motility *in ovo* and electrical bursting activity *in vitro*, which were associated with the correlated wave generated in the brain, were transiently increased, but subsequently inhibited by nicotine (Figs. 1C and 2), the latter of which may have been due to the desensitization of nAChRs and/or desynchronization of neurons recruited into the wave. The results suggest that the positive effects of nicotine on the wave were transient, and the dominant action was to inhibit the wave.

In a previous study by Ejaz and Woong (2006), side stream whole smoke solutions were applied to E7 embryos *in ovo*, which markedly reduced embryonic motility. Nicotine, the main toxicant involved in the smoke solution, was suggested to be responsible for the reduction in embryonic motility. The present study provides direct experimental support for this hypothesis.

In a study performed on the embryonic chick spinal cord at later developmental stages (E10), nicotine increased the frequency of spontaneous activity by enhancing GABA (excitatory at this stage) release from Renshow cells (Gonzalez-Islas et al., 2016). The collateral circuit *via* the Renshow cell has not differentiated at E5-E6 (Mochida et al., 2001). Furthermore, E10 is a stage at which spontaneous activity originating in the spinal cord no longer exhibits “large-scale” propagation invading the brain, but is segregated in the spinal cord (Momose-Sato and Sato, 2014), and the dominant transmitter mediating this activity is not acetylcholine, but glutamate (Chub and O’Donovan, 1998; Mochida

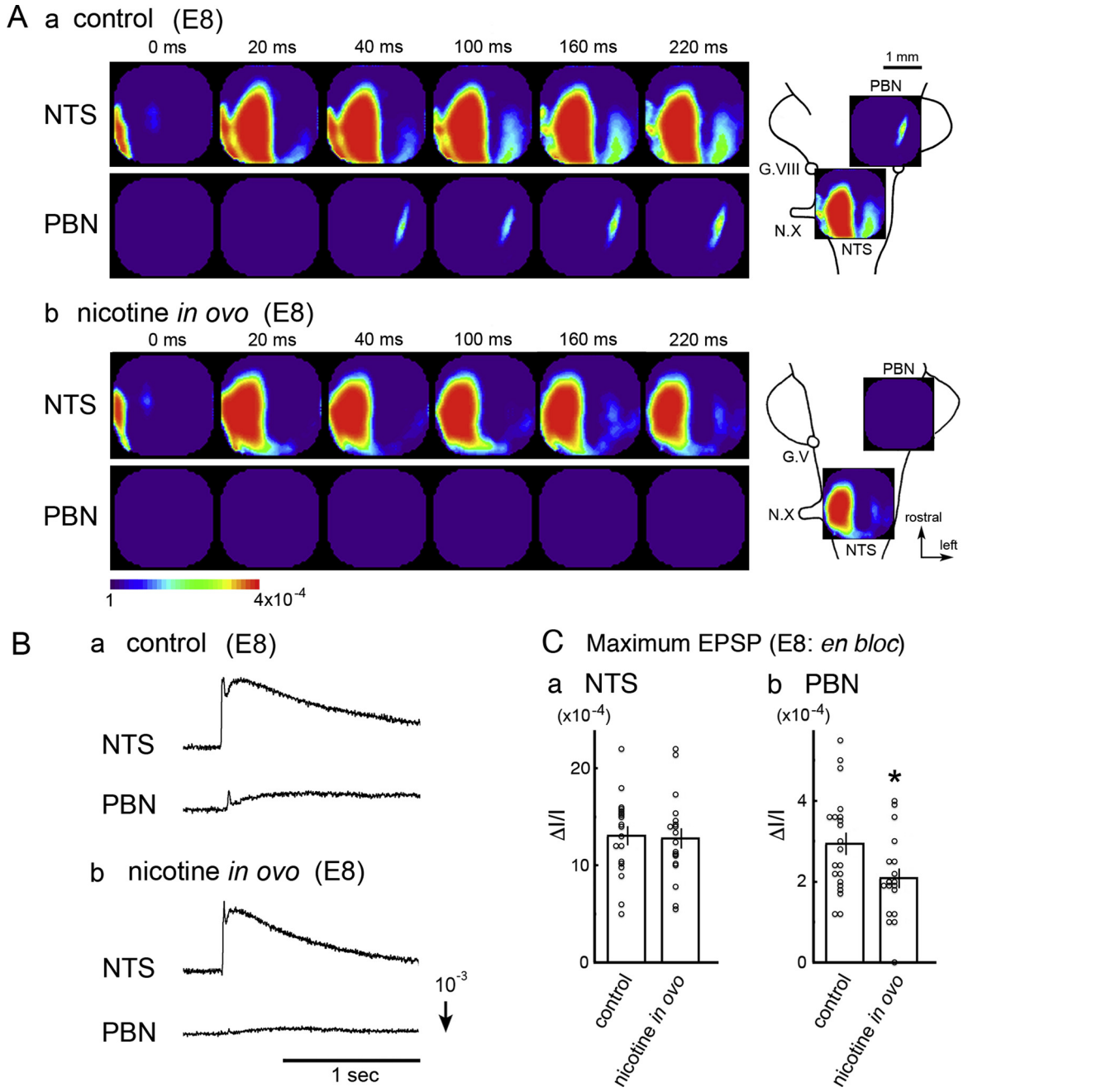

Fig. 4. Evaluation of chronic exposure to nicotine on vagal polysynaptic responses.
A, Pseudocolor images of vagal responses in E8 *en bloc* brainstem preparations dissected from embryos with (**b**) or without (**a**) chronic exposure to nicotine *in ovo* (5 mM, 100 μL/day). The upper and lower images were obtained from the ipsilateral NTS and contralateral PBN, respectively. The frame interval was 20–60 msec. The recorded areas are indicated in the right insets with the sixth images overlapped on the preparation. G.V, trigeminal ganglion; G.VIII, vestibulo-cochlear ganglion; N.X, vagus nerve. **B,** Enlarged traces of optical signals detected from the ipsilateral NTS (upper traces) and contralateral PBN (lower traces) in E8 preparations. The recordings were obtained with (**b**) or without (**a**) the application of nicotine *in ovo*. **C,** Histograms showing the maximum amplitude of the EPSP-related slow signal (mean ± SEM) together with each data point (circles) in the NTS (**a**) and PBN (**b**) of E8 *en bloc* brainstems. "*" shows that the effects of nicotine were significant ($P < 0.05$).

et al., 2009). Thus, difficulties are associated with comparing results between studies performed at different stages.

4.2. Nicotine disrupted synaptic network formation

The chronic application of nicotine *in ovo* did not significantly affect monosynaptic EPSPs in the first-order nucleus of the vagal sensory pathway, the NTS, or the contralateral non-NTS region. However, it markedly reduced polysynaptic EPSPs in the higher-order sensory nucleus, the PBN. These results are consistent with previous findings obtained using other blockers of correlated wave activity, bicuculline/strychnine and *d*-tubocurarine (Momose-Sato and Sato, 2017), indicating that the effects of nicotine on the EPSP were not due to the toxic effects of the drug, but to the inhibition of correlated wave activity. The present results showed that nicotine disrupted synaptic network formation along the sensory pathway by inhibiting correlated spontaneous activity.

Regarding monosynaptic EPSPs in the first-order nucleus not being

affected by the loss of correlated wave activity, we previously suggested that synaptic functions in the first-order nucleus did not appear to be under the control of the correlated wave (Momose-Sato and Sato, 2017). Pre- and postsynaptic neurons in the PBN (NTS neurons innervating the PBN and PBN neurons receiving the innervation, respectively) may be spontaneously co-activated with the correlated wave. However, this was not the case in the NTS and contralateral region because the presynaptic neurons innervating these nuclei are located outside the brain and not recruited into the wave. The coincident activation of pre- and postsynaptic components has been shown to strengthen and stabilize synapses (Murphy, 2003). This activity-dependent mechanism may contribute to the process of functional synapse formation regulated by correlated wave activity. The molecular and electrophysiological mechanisms involved and how neural networks are modified currently remain unclear. Disruption of the wave may have inhibited synaptogenesis or other processes of neural network formation, including axon elongation. Previous studies reported that spontaneous activity in the spinal cord regulates motoneuronal axon pathfinding (Hanson and Landmesser, 2004; Kastanenka and Landmesser, 2010). Therefore, the elongation and innervation of presynaptic fibers along the sensory pathway may be regulated by spontaneous wave activity.

4.3. Clinical considerations

Numerous human and animal studies have confirmed that nicotine exposure during pregnancy causes a spectrum of fetal and infant deficits, including fetal growth retardation, stillbirth, and sudden infant death syndrome (SIDS) (Thompson et al., 2009; Li et al., 2012). In addition to the abnormalities in pregnancy outcomes and neonatal mortality, nicotine causes long-term neurological deficits, including impaired cognitive function, attention deficit hyperactivity disorder (ADHD), disorders of respiratory responses, and varying levels of motor and sensory deficiencies (Thompson et al., 2009; Li et al., 2012). Nicotine exerts its effects by interacting with nAChRs, which are known to influence signaling molecules and developmental processes by increasing $[Ca^{2+}]_i$, and regulating gene expression, cell death, synaptogenesis, and plasticity events (Nguyen et al., 2001; Dajas-Bailador and Wonnacott, 2004). The present study demonstrated that the inhibition of correlated wave activity and subsequent retardation of synaptic network formation were detrimental effects of prenatal nicotine exposure.

Embryonic motility similar to that observed in the chick embryo *in ovo* and rodent fetuses *in utero* has been detected in human fetuses as early as 5–5.5 weeks (postconceptional age) (de Vries et al., 1982; Lüchinger et al., 2008; O'Rahilly and Müller, 2008). Since the effects of nicotine on correlated wave activity were similar among chick, mouse, and rat embryos (Fig. 2), maternal cigarette smoking may affect synaptic network formation in human fetuses by interfering with correlated activity. In order to test this hypothesis, it is important to confirm whether correlated activity in mammals has a similar fundamental role in synaptic network formation, as demonstrated in the chick embryo, and also if prenatal nicotine exposure interferes with this developmental process *in situ*. Future studies that target sensory pathways other than the vagal system will also be beneficial for confirmed whether the results obtained in the present study are common in other sensory systems recruited into the correlated wave.

Conflict of interest

None.

CRediT authorship contribution statement

Yoko Momose-Sato: Investigation, Formal analysis, Visualization, Writing - original draft, Funding acquisition. **Katsushige Sato:** Investigation, Formal analysis, Visualization, Writing - review & editing, Funding acquisition.

Acknowledgement

This work was supported by grants 19K06962 (Y. Momose-Sato) and 18K06530 (K. Sato) from the Japan Society for the Promotion of Science.

Appendix A. Supplementary data

Supplementary material related to this article can be found, in the online version, at doi:https://doi.org/10.1016/j.ibror.2020.06.003.

References

Bekoff, A., Stein, P.S.G., Hamburger, V., 1975. Coordinated motor output in the hindlimb of the 7-day chick embryo. Proc. Nat. Acad. Sci. U. S. A. 72, 1245–1248.
Branchereau, P., Morin, D., Bonnot, A., Ballion, B., Chapron, J., Viala, D., 2000. Development of lumbar rhythmic networks: from embryonic to neonate locomotor-like patterns in the mouse. Brain Res. Bull. 53, 711–718.
Chub, N., O'Donovan, M., 1998. Blockade and recovery of spontaneous rhythmic activity after application of neurotransmitter antagonists to spinal networks of the chick embryo. J. Neurosci. 18, 294–306.
Corner, M.A., 1977. Sleep and the beginnings of behavior in the animal kingdom – studies of ultradian motility cycles in early life. Prog. Neurobiol. 8, 279–295.
Dajas-Bailador, F., Wonnacott, S., 2004. Nicotinic acetylcholine receptors and the regulation of neuronal signalling. Trends Pharmacol. Sci. 25, 317–324.
Dani, J.A., Bertrand, D., 2007. Nicotinic acetylcholine receptors and nicotinic cholinergic mechanisms of the central nervous system. Annu. Rev. Pharmacol. Toxicol. 47, 699–729.
de Vries, J.I.P., Visser, G.H.A., Prechtl, H.F.R., 1982. The emergence of fetal behaviour. I. Qualitative aspects. Early Human Dev. 7, 301–322.
Dwyer, J.B., McQuown, S.C., Leslie, F.M., 2009. The dynamic effects of nicotine on the developing brain. Pharmacol. Therapeutics 122, 125–139.
Ejaz, S., Woong, L.C., 2006. Diminished embryonic movements of developing embryo by direct exposure of sidestream whole smoke solutions. Arch. Toxicol. 80, 107–114.
Glover, J.C., Sato, K., Momose-Sato, Y., 2008. Using voltage-sensitive dye recording to image the functional development of neuronal circuits in vertebrate embryos. Dev. Neurobiol. 68, 804–816.
Gonzalez-Islas, C., Wenner, P., 2006. Spontaneous network activity in the embryonic spinal cord regulates AMPAergic and GABAergic synaptic strength. Neuron 49, 563–575.
Gonzalez-Islas, C., Garcia-Bereguiain, M.A., O'Flaherty, B., Wenner, P., 2016. Tonic nicotinic transmission enhances spinal GABAergic presynaptic release and the frequency of spontaneous network activity. Dev. Neurobiol. 76, 298–312.
Hall, B.K., Herring, S.W., 1990. Paralysis and growth of the musculoskeletal system in the embryonic chick. J. Morphol. 206, 45–56.
Hamburger, V., Balaban, M., 1963. Observations and experiments on spontaneous rhythmical behavior in the chick embryo. Dev. Biol. 7, 533–545.
Hanson, M.G., Landmesser, L.T., 2004. Normal patterns of spontaneous activity are required for correct motor axon guidance and the expression of specific guidance molecules. Neuron 43, 687–701.
Heindel, J.J., Balbus, J., Birnbaum, L., Brune-Drisse, M.N., Grandjeam, P., Gray, K., Landrigan, P.J., Sly, P.D., Suk, W., Slechta, D.C., Thompson, C., Hanson, M., 2015. Developmental origin of health and disease: integrating environmental influences. Endocrinology 156, 3416–3421.
Herbert, H., Moga, M.M., Saper, C.B., 1990. Connections of the parabrachial nucleus with the nucleus of the solitary tract and the medullary reticular formation in the rat. J. Comp. Neurol. 293, 540–580.
Hirota, A., Sato, K., Momose-Sato, Y., Sakai, T., Kamino, K., 1995. A new simultaneous 1020-site optical recording system for monitoring neural activity using voltage-sensitive dyes. J. Neurosci. Meth. 56, 187–194.
Kamino, K., 1991. Optical approaches to ontogeny of electrical activity and related functional organization during early heart development. Physiol. Rev. 71, 53–91.
Kamino, K., Hirota, A., Fujii, S., 1981. Localization of pacemaking activity in early embryonic heart monitored using voltage-sensitive dye. Nature 290, 595–597.
Kamino, K., Hirota, A., Komuro, H., 1989. Optical indications of electrical activity and excitation-contraction coupling in the early embryonic heart. Adv. Biophys. 25, 45–93.
Kastanenka, K.V., Landmesser, L.T., 2010. In vivo activation of channelrhodopsin-2 reveals that normal patterns of spontaneous activity are required for motoneuron guidance and maintenance of guidance molecules. J. Neurosci. 30, 10575–10585.
Komuro, H., Sakai, T., Momose-Sato, Y., Hirota, A., Kamino, K., 1991. Optical detection of postsynaptic potentials evoked by vagal stimulation in the early embryonic chick brain stem slice. J. Physiol. (Lond.) 442, 631–648.
Ladle, D.R., Pecho-Vrieseling, E., Arber, S., 2007. Assembly of motor circuits in the spinal cord: driven to function by genetic and experience-dependent mechanisms. Neuron 56, 270–283.
Lee, M.T., Koebbe, M.J., O'Donovan, M.J., 1988. The development of sensorimotor synaptic connections in the lumbosacral cord of the chick embryo. J. Neurosci. 8,

2530–2543.
Li, Y., Gonzalez, P., Zhang, L., 2012. Fetal stress and programming of hypoxic/ischemic-sensitive phenotype in the neonatal brain: mechanisms and possible interventions. Prog. Neurobiol. 98, 145–165.
Lüchinger, A.B., Hadders-Algra, M., van Kan, C.M., de Vries, J.I.P., 2008. Fetal onset of general movements. Pediatr. Res. 63, 191–195.
Milner, L.D., Landmesser, L.T., 1999. Cholinergic and GABAergic inputs drive patterned spontaneous motoneuron activity before target contact. J. Neurosci. 19, 3007–3022.
Mochida, H., Sato, K., Arai, Y., Sasaki, S., Yazawa, I., Kamino, K., Momose-Sato, Y., 2001. Multiple-site optical recording reveals embryonic organization of synaptic networks in the chick spinal cord. Eur. J. Neurosci. 13, 1547–1558.
Mochida, H., Sato, K., Momose-Sato, Y., 2009. Switching of the transmitters that mediate hindbrain correlated activity in the chick embryo. Eur. J. Neurosci. 29, 14–30.
Momose-Sato, Y., Sato, K., 2005. Primary vagal projection to the contralateral non-NTS region in the embryonic chick brainstem revealed by optical recording. J. Memb. Biol. 208, 183–191.
Momose-Sato, Y., Sato, K., 2006. Optical recording of vagal pathway formation in the embryonic brainstem. Auto. Neurosci.: Basic Clin. 126–127, 39–49.
Momose-Sato, Y., Sato, K., 2011. The embryonic brain and development of vagal pathways. Resp. Physiol. Neurobiol. 178, 163–173.
Momose-Sato, Y., Sato, K., 2013. Large-scale synchronized activity in the embryonic brainstem and spinal cord. Front. Cell. Neurosci. 7, 1–15 Article 36.
Momose-Sato, Y., Sato, K., 2014. Maintenance of the large-scale depolarization wave in the embryonic chick brain against deprivation of the rhythm generator. Neuroscience 266, 186–196.
Momose-Sato, Y., Sato, K., 2016a. Development of spontaneous activity in the avian hindbrain. Front. Neural Circuits 10, 1–5 Article 63.
Momose-Sato, Y., Sato, K., 2016b. Development of synaptic networks in the mouse vagal pathway revealed by optical mapping with a voltage-sensitive dye. Eur. J. Neurosci. 44, 1906–1918.
Momose-Sato, Y., Sato, K., 2017. Developmental roles of the spontaneous depolarization wave in synaptic network formation in the embryonic brainstem. Neuroscience 365, 33–47.
Momose-Sato, Y., Sato, K., 2019. Exposure to nicotine during development disrupts synaptic network formation by inhibiting correlated spontaneous wave activity. Soc. Neurosci. 49th Ann. Meeting Abst.
Momose-Sato, Y., Sakai, T., Komuro, H., Hirota, A., Kamino, K., 1991. Optical mapping of the early development of the response pattern to vagal stimulation in embryonic chick brain stem. J. Physiol. (Lond.) 442, 649–668.
Momose-Sato, Y., Sakai, T., Hirota, A., Sato, K., Kamino, K., 1994. Optical mapping of early embryonic expressions of Mg^{2+}-/APV-sensitive components of vagal glutaminergic EPSPs in the chick brainstem. J. Neurosci. 14, 7572–7584.
Momose-Sato, Y., Sato, K., Sakai, T., Hirota, A., Matsutani, K., Kamino, K., 1995. Evaluation of optimal voltage-sensitive dyes for optical monitoring of embryonic neural activity. J. Memb. Biol. 144, 167–176.
Momose-Sato, Y., Sato, K., Kamino, K., 2001. Optical approaches to embryonic development of neural functions in the brainstem. Prog. Neurobiol. 63, 151–197.
Momose-Sato, Y., Sato, K., Kinoshita, M., 2007. Spontaneous depolarization waves of multiple origins in the embryonic rat CNS. Eur. J. Neurosci. 25, 929–944.
Momose-Sato, Y., Mochida, H., Kinoshita, M., 2009. Origin of the earliest correlated neuronal activity in the chick embryo revealed by optical imaging with voltage-sensitive dyes. Eur. J. Neurosci. 29, 1–13.
Momose-Sato, Y., Nakamori, T., Sato, K., 2012a. Spontaneous depolarization wave in the mouse embryo: origin and large-scale propagation over the CNS identified with voltage-sensitive dye imaging. Eur. J. Neurosci. 35, 1230–1241.
Momose-Sato, Y., Nakamori, T., Sato, K., 2012b. Pharmacological mechanisms underlying the switching from the large-scale depolarization wave to segregated activity in the mouse CNS. Eur. J. Neurosci. 35, 1242–1252.
Momose-Sato, Y., Sato, K., Kamino, K., 2015. Monitoring population membrane potential signals during development of the vertebrate nervous system. In: Canepari, M., Zecevic, D., Bernus, O. (Eds.), Membrane Potential Imaging in the Nervous System and in the Heart. Springer, New York, pp. 213–242.
Murphy, T.H., 2003. Activity-dependent synapse development: changing the rules. Nat. Neurosci. 6, 9–11.
Myers, C.P., Lewcock, J.W., Hanson, M.G., Gosgnach, S., Aimone, J.B., Gage, F.H., Lee, K.-F., Landmesser, L.T., Pfaff, S.L., 2005. Cholinergic input is required during embryonic development to mediate proper assembly of spinal locomotor circuits. Neuron 46, 37–49.
Nakayama, K., Nishimaru, H., Iizuka, M., Ozaki, S., Kudo, N., 1999. Rostrocaudal progression in the development of periodic spontaneous activity in fetal rat spinal motor circuits in vitro. J. Neurophysiol. 81, 2592–2595.
Nguyen, L., Rigo, J.-M., Rocher, V., Belachew, S., Malgrange, B., Rogister, B., Leprince, P., Moonen, G., 2001. Neurotransmitters as early signals for central nervous system development. Cell Tissue Res. 305, 187–202.
Norgren, R., 1978. Projections from the nucleus of the solitary tract in the rat. Neuroscience 3, 207–218.
O'Donovan, M.J., 1999. The origin of spontaneous activity in developing networks of the vertebrate nervous system. Curr. Opin. Neurobiol. 9, 94–104.
O'Rahilly, R., Müller, F., 2008. Significant features in the early prenatal development of the human brain. Ann. Anat. 190, 105–118.
Obaid, A.L., Orkand, R.K., Gainer, H., Salzberg, B.M., 1985. Active calcium responses recorded optically from nerve terminals of the frog neurohypophysis. J. Gen. Physiol. 85, 481–489.
Orbach, H.S., Cohen, L.B., Grinvald, A., 1985. Optical mapping of electrical activity in rat somatosensory and visual cortex. J. Neurosci. 5, 1886–1895.
Persson, M., 1983. The role of movements in the development of sutural and diarthrodial joints tested by long-term paralysis of chick embryos. J. Anat. 137, 591–599.
Provine, R.R., 1973. Neurophysiological aspects of behavior development in the chick embryo. In: In: Gottlieb, G. (Ed.), Studies on the Development of Behavior and the Nervous System, Behavioral Embryology 1. Academic Press, New York, pp. 77–102.
Ren, J., Greer, J.J., 2003. Ontogeny of rhythmic motor patterns generated in the embryonic rat spinal cord. J. Neurophysiol. 89, 1187–1195.
Ross, W.N., Salzberg, B.M., Cohen, L.B., Grinvald, A., Davila, H.V., Waggoner, A.S., Wang, C.H., 1977. Changes in absorption, fluorescence, dichroism, and birefringence in stained ginat axons: optical measurement of membrane potential. J. Memb. Biol. 33, 141–183.
Roufa, D., Martonosi, A.N., 1981. Effect of curare on the development of chicken embryo skeletal muscle in ovo. Biochem. Pharmacol. 30, 1501–1505.
Salzberg, B.M., Grinvald, A., Cohen, L.B., Davila, H.V., Ross, W.N., 1977. Optical recording of neuronal activity in an invertebrate central nervous system: simultaneous monitoring of several neurons. J. Neurophysiol. 40, 1281–1291.
Salzberg, B.M., Obaid, A.L., Senseman, D.M., Gainer, H., 1983. Optical recording of action potentials from vertebrate nerve terminals using potentiometric probes provides evidence for sodium and calcium components. Nature 306, 36–40.
Sato, K., Miyakawa, N., Momose-Sato, Y., 2004. Optical survey of neural circuit formation in the embryonic chick vagal pathway. Eur. J. Neurosci. 19, 1217–1225.
Sato, K., Momose-Sato, Y., Sakai, T., Hirota, A., Kamino, K., 1995. Responses to glossopharyngeal stimulus in the early embryonic chick brainstem: Spatiotemporal patterns in three dimensions from repeated multiple-site optical recording of electrical activity. J. Neurosci. 15, 2123–2140.
Slotkin, T.A., 2004. Cholinergic systems in brain development and disruption by neurotoxicants: nicotine, environmental tobacco smoke, organophosphates. Toxicol. Appl. Pharmacol. 198, 132–151.
Thoby-Brisson, M., Trinh, J.-B., Champagnat, J., Fortin, G., 2005. Emergence of the pre-Bötzinger respiratory rhythm generator in the mouse embryo. J. Neurosci. 25, 4307–4318.
Thoby-Brisson, M., Karlén, M., Wu, N., Charnay, P., Champagnat, J., Fortin, G., 2009. Genetic identification of an embryonic parafacial oscillator coupling to the pre-Bötzinger complex. Nat. Neurosci. 12, 1028–1036.
Thompson, B.L., Levitt, P., Stanwood, G.D., 2009. Prenatal exposure to drugs: effects on brain development and implications for policy and education. Nat. Rev. Neurosci. 10, 303–312.
Vincen-Brown, M.A., Revill, A.L., Pilarski, J.Q., 2016. Activity-dependent plasticity in the isolated embryonic avian brainstem following manipulations of rhythmic spontaneous neural activity. Resp. Physiol. Neurobiol. 229, 24–33.
Wilhelm, J.C., Rich, M.M., Wenner, P., 2009. Compensatory changes in cellular excitability, not synaptic scaling, contribute to homeostatic recovery of embryonic network activity. Proc. Nat. Acad. Sci. U. S. A. 106, 6760–6765.
Wong, R.O.L., 1999. Retinal waves and visual system development. Ann. Rev. Neurosci. 22, 29–47.